

1 **Impact of cooking style and oil on semi-volatile and intermediate**
2 **volatility organic compound emissions from Chinese domestic cooking**

3 Kai Song^{1,2}, Song Guo^{1,2,*}, Yuanzheng Gong¹, Daqi Lv¹, Yuan Zhang^{1,3}, Zichao Wan¹, Tianyu Li¹,
4 Wenfei Zhu¹, Hui Wang¹, Ying Yu¹, Rui Tan¹, Ruizhe Shen¹, Sihua Lu¹, Shuangde Li⁴, Yunfa Chen⁴,
5 Min Hu^{1,2}

6
7
8 ¹ State Key Joint Laboratory of Environmental Simulation and Pollution Control, International Joint
9 Laboratory for Regional Pollution Control, Ministry of Education (IJRC), College of Environmental
10 Sciences and Engineering, *Beijing* 100871, China

11 ² Collaborative Innovation Center of Atmospheric Environment and Equipment Technology, Nanjing
12 University of Information Science & Technology, *Nanjing* 210044, China

13 ³ School of Earth Science and Engineering, Hebei University of Engineering, *Handan* 056038, China.

14 ⁴ State Key Laboratory of Multiphase Complex Systems, Institute of Process Engineering, Chinese
15 Academy of Sciences, *Beijing* 100190, China

16 * **Correspondence:** Song Guo: songguo@pku.edu.cn

17

18

19 **Abstract:**

20 To elucidate the molecular chemical compositions, volatility-polarity distributions, as well as
21 influencing factors of Chinese cooking emissions, a comprehensive cooking emission experiment
22 was conducted. Volatile organic compounds (VOCs), intermediate volatility, and semi-volatile
23 organic compounds (I/SVOCs) from cooking fumes were analyzed by a thermal desorption
24 comprehensive two-dimensional gas chromatography coupled with quadrupole mass spectrometer
25 (TD-GC×GC-qMS). Emissions from four typical Chinese dishes, i.e., fried chicken, Kung Pao
26 chicken, pan-fried tofu, and stir-fried cabbage were investigated to illustrate the impact of cooking
27 style and material. Fumes of chicken fried with corn, peanut, soybean, and sunflower oils were
28 investigated to demonstrate the influence of cooking oil. A total of 201 chemicals were quantified.
29 Kung Pao chicken emitted more pollutants than other dishes due to its rather intense cooking method.
30 Aromatics and oxygenated compounds were extensively detected among meat-related cooking fumes,
31 while a vegetable-related profile was observed in the emissions of stir-fried cabbage. Ozone
32 formation potential (OFP) was dominated by chemicals in the VOC range. 10.2% - 32.0% of the
33 SOA estimation could be explained by S/IVOCs. Pixel-based partial least squares-discriminant
34 analysis (PLS-DA) and multiway principal component analysis (MPCA) were utilized for sample
35 classification and component identification. The results indicated that the oil factor explained more
36 variance of chemical compositions than the cooking style factor. MPCA results emphasize the
37 importance of the unsaturated fatty acid-alkadienal-volatile products mechanism (oil autooxidation)
38 accelerated by the cooking and heating procedure.

39

40 **Keywords:** Cooking emissions; Semi-volatile organic compounds; Intermediate volatility organic
41 compounds; Cooking style; Oil

42

43

44

45

46

47 **1 Introduction**

48 Organics are key components of urban particles (Guo et al., 2014; Tang et al., 2018). Source
49 apportionment results indicated that vehicle exhaust is one of the important sources of gaseous and
50 particulate organics (Guo et al., 2012, 2020; Hu et al., 2015; Wang et al., 2021). However, the
51 importance of cooking emissions is rising due to the high impact on both primary precursor
52 emissions and secondary formation (Zhu et al., 2021). Cooking emitted organics are complex
53 mixtures covering a wide range of volatility, including volatile organic compounds (VOCs, organics
54 with effective saturation concentration higher than $10^6 \mu\text{g m}^{-3}$) (Bruns et al., 2016; Fullana et al.,
55 2004; Huang et al., 2011; Lu et al., 2021; Zhang et al., 2019), intermediate volatility organic
56 compounds (IVOCs, organics with effective saturation concentration in the range of $10^3 - 10^6 \mu\text{g m}^{-3}$)
57 (Liu et al., 2018; Lu et al., 2021; Schauer et al., 2002), and semi-volatile organic compounds
58 (SVOCs, organics with effective saturation concentration in the range of $10^{-1} - 10^3 \mu\text{g m}^{-3}$) (Liu et al.,
59 2018; Lu et al., 2021; Ma et al., 2021; Schauer et al., 2002; Vicente et al., 2021; Yu et al., 2021).
60 Along with a large variety of volatility, these organics are also a large pool of complex components
61 of different polarities, such as alkanes with lower polarity (Gysel et al., 2018; Lin et al., 2010; Wang
62 et al., 2015), polycyclic aromatics with intermediate polarity (Chen et al., 2019; Kim et al., 2013;
63 Wei See et al., 2006), acids, ketones, and aldehydes with higher polarity (Alves et al., 2012; Gysel et
64 al., 2018; He et al., 2004; Peng et al., 2017). Such cooking-related organics are key pollutants
65 exhibiting health effects (Gligorovski et al., 2018; Huang et al., 2011; Zhao and Zhao, 2018) and air-
66 quality problems (Abdullahi et al., 2013; Zhao and Zhao, 2018). Although chemical compositions,
67 fingerprints, and influencing factors of cooking emissions have been investigated in some previous
68 studies (Alves et al., 2021; Klein et al., 2016a; Peng et al., 2017; Vicente et al., 2021), there are still
69 questions that remain uncertain. The first constraint is that resolving complex mixtures of cooking
70 emissions is rather tough. Most components in traditional gas chromatography-mass spectrometer
71 (GC-MS) chromatograms remain unresolved (Takhar et al., 2021; Zhao et al., 2014). It is of vital
72 importance to identify chemical compositions of unresolved complex mixtures (UCM) to better
73 understand their contributions to secondary organic aerosol (SOA). For instance, Huo et al
74 investigated the S/IVOC emissions from incomplete combustion utilizing GC \times GC-MS. They found

75 that the previous bins-based method caused SOA underestimation with the ratio of $62.5 \pm 25.2\%$ to
76 $80.9 \pm 2.8\%$ (Huo et al., 2021). Particle-phase SVOC organics from cooking emissions are widely
77 demonstrated yet few studies focus on gas-phase IVOC or SVOC organics. Meanwhile, current
78 studies mainly focus on a single kind or a series of homologs (aldehydes (Abdullahi et al., 2013;
79 Klein et al., 2016a; Peng et al., 2017), alkanes (Abdullahi et al., 2013), or acids (Abdullahi et al.,
80 2013; Takhar et al., 2021; Zeng et al., 2020)). In other words, currently, there are few comprehensive
81 source profiles of cooking emissions covering VOCs, IVOCs, and SVOCs (Schauer et al., 1999; Yu
82 et al., 2022).

83 The volatility-based method originated from the volatility-based set (VBS) is widely used to
84 demonstrate IVOC or SVOC emissions from different sources (Zhao et al., 2014, 2017), yet
85 chemical compositions from cooking emissions could not be demonstrated well only from the
86 volatility perspective. Large proportions of acids, esters, polycyclic aromatic hydrocarbons (PAHs),
87 and *n*-alkanes expand a wide range of polarity. A novel scheme combining volatility and polarity
88 should be developed to better identify source emission characteristics.

89 Besides, it is well-known that cooking emissions vary dramatically with cooking style,
90 ingredients, food, oil, and temperature (Amouei Torkmahalleh et al., 2017; Klein et al., 2016b; Liu et
91 al., 2018; Takhar et al., 2021; Zhao et al., 2007b). Cooking style and oil are typical influencing
92 factors dominating the compositions of cooking fume (Klein et al., 2016a; Takhar et al., 2021; Zhang
93 et al., 2019). Some studies demonstrated the emission patterns of cooking fumes emphasizing the
94 influence of different dishes or cooking methods (Chen et al., 2018; Wang et al., 2020), and several
95 studies clarified the importance of *n*-alkanes (Zhao et al., 2007a), polycyclic aromatic hydrocarbons
96 (PAHs) (Abdel-Shafy and Mansour, 2016; Abdullahi et al., 2013), aldehydes (Katragadda et al., 2010;
97 Peng et al., 2017), and acids (Pei et al., 2016; Zeng et al., 2020; Zhao et al., 2007a) from cooking
98 emissions using various kinds of oils. However, few comprehensive investigations have been
99 reported that speculated the dominant influencing factor under multiple conditions of cooking
100 procedures.

101 In this work, a thermal desorption comprehensive two-dimensional gas chromatography
102 coupled with quadrupole mass spectrometer (TD-GC×GC-qMS) is utilized to resolve and quantify

103 gaseous organic emissions from the molecular level. GC×GC has been proved to be a powerful
104 technique to resolve UCM in previous studies (Cordero et al., 2018; Zhang et al., 2021a). A two-
105 dimensional panel combining the volatility and polarity properties of chemicals is developed to
106 better understand organic emissions. The ozone formation potential (OFP) and SOA formation from
107 gaseous precursors were estimated. To elucidate the main influencing factor of cooking emissions,
108 pixel-based partial least squares-discriminant analysis (PLS-DA) was utilized. The main chemical
109 reactions of cooking emission were further inferred by pixel-based multiway principal component
110 analysis (MPCA).

111 **2 Experimental description**

112 **2.1 Sampling and quantification**

113 Four typical Chinese dishes, i.e., fried chicken, Kung Pao chicken, pan-fried tofu, and stir-fried
114 cabbage, were cooked in corn oil in the laboratory of the Institute of Process Engineering, Chinese
115 Academy of Sciences. The detailed cooking procedures could be found in Table S1 and elsewhere
116 (Zhang et al., 2021b). Meanwhile, four types of oil (i.e., soybean, corn, sunflower, and peanut oil)
117 were used for frying chicken to illustrate the influence of oil. These four oils were chosen for
118 chicken-frying as they are commonly consumed in China (especially soybean oil) (Jamet and
119 Chaumet, 2016) and other countries worldwide (Awogbemi et al., 2019).

120 Cooking fumes were sampled directly without dilution. After collecting particles on quartz
121 filters, gas-phase organics were sampled by pre-conditioned Tenax TA tubes (Gerstel 6 mm 97 OD,
122 4.5 mm ID glass tube filled with ~290 mg Tenax TA) with a flow of 0.5 L min⁻¹. The removal of
123 particles on the quartz filter in front of the Tenax TA tubes affects the S/IVOC measurements,
124 causing positive and negative artifacts. Some of the gaseous SVOCs could be lost to sorption onto
125 filters, and some particle-phase SVOCs could evaporate off the filter. The emission pattern of the
126 particulate organics diverged from gas-phase organics, and a small overlap of species is identified.
127 Aromatics, aldehydes, and short-chain acids mainly occurred in the gas-phase. For instance, the
128 detection of short-chain olefinic aldehydes in the gas-phase was 40 times that of the particle-phase
129 aldehydes. The artifacts of particulates on gas-phase aromatics and oxygenated compounds could be
130 less than 5%. A typical system blank chromatogram is displayed in Figure S1. A daily blank

131 sampling of the air in the kitchen ventilator was conducted before cooking and was subtracted in the
132 quantification procedure. The sampling time in this work is 15 ~ 30 min (0.5 L min^{-1}). All samples
133 were frozen at -20°C before analyzing. A Tenax TA breakthrough experiment was conducted by
134 sampling two adsorbent tubes in series. We sampled the first tube (sample tube) and the second tube
135 (backup tube) simultaneously with a sampling time of 24h. No breakthrough was observed after 24h
136 sampling (Figure S2). The total intensity of cooking emission chromatograms ($3.05 \times 10^9 - 14.17 \times$
137 10^9) falls in the range of the sample tube (9.84×10^9), which was much higher than the intensity of
138 the backup tube (2.12×10^9) and the blank tube (1.33×10^9 , Figure S1). After subtracting the volume
139 of the blank tube, the volume of the backup tube is less than 10% of the sample tube, indicating the
140 breakthrough effect of the Tenax TA tubes could be neglected.

141 A thermal desorption comprehensive two-dimensional gas chromatography coupled with
142 quadrupole mass spectrometer (TD-GC \times GC-qMS, GC-MS TQ8050, Shimadzu, Japan) was utilized
143 for sample analysis with a desorption temperature of 280°C . The modulation period was 6s. See
144 more detail in Table S2. As the first and second columns of GC \times GC were non-polar SH-Rxi-1ms (30
145 $\text{m} \times 0.25 \text{ mm} \times 0.25 \mu\text{m}$) and mid-polar BPX50 ($2.5 \text{ m} \times 0.1 \text{ mm} \times 0.1 \mu\text{m}$), the 1st retention time of
146 a chemical is related to its volatility while 2nd retention time is related to polarity (Nabi et al., 2014;
147 Nabi and Arey, 2017; Zushi et al., 2016). The total chromatogram was cut into volatility bins (B8 to
148 B31 with a decrease in volatility) following the pipeline of previous studies (Tang et al., 2021; Zhao
149 et al., 2014, 2017, 2018), while it was cut into slices by an increase of 0.5 s in the second retention
150 time (called 2D bins, from P1 to P12 with an increase of polarity). For instance, C12 lies in B12
151 (saturated vapor concentration $\sim 10^6 \mu\text{g m}^{-3}$, IVOC range) and P2 bins (low polarity). Benzophenone
152 lies in B16 (saturated vapor concentration $\sim 10^5 \mu\text{g m}^{-3}$, IVOC range) and P6 bins (medium to high
153 polarity). A two-dimensional panel was developed in this way to investigate the emission of
154 contaminants from aspects of their volatility and polarity properties (Song et al., 2022).

155 326 chemicals were quantified (Table S3) while 201 contaminants were detected (Table S4) in
156 cooking fumes covering a wide range of VOCs, IVOCs, and SVOCs, including 25 aromatics, 19 *n*-
157 alkanes, 100 oxygenated compounds (containing 7 acids, 10 alcohols, 29 aldehydes, 24 esters, 5
158 ketones, and others), 3 PAHs, and 54 other chemicals. The 1D retention time shift of most chemicals

159 is within 0.5 min, while the 2D retention time shift of most chemicals is within 0.1s (Table S4),
160 which is much less than the length of 1D (~ 8 min) and 2D (0.5s) bins. Most of the R^2 of external
161 calibration curves was between 0.90 – 1 (Table S5). Chemicals without standards are semi-quantified
162 by surrogates from the same class or *n*-alkanes in the same 1D bins (Table S3). The uncertainties of
163 semi-quantification of surrogates from the same class or *n*-alkanes were 27% and 69% (Table S6).
164 The average emission rates ($\mu\text{g min}^{-1}$) of (semi-)quantified chemicals are listed in Table S4.

165 Quartz filters added with about 1 mL of edible oils were also thermally desorbed and analyzed
166 by TD-GC×GC-qMS. The total responses of blobs are normalized to 1 and the results were given by
167 percent response (%).

168 **2.2 Emission rate calculation, estimation of ozone and secondary organic aerosol (SOA)** 169 **formation potential**

170 Emission rate (ER , $\mu\text{g min}^{-1}$) was calculated by the following equation, where c is the blank
171 subtracted mass concentration ($\mu\text{g m}^{-3}$) of the chemical quantified, and Q is the mass flow of cooking
172 exhaust emissions ($15 \text{ m}^3 \text{ min}^{-1}$).

$$173 \quad \text{ER} = c \times Q \quad (1)$$

174 Ozone formation potential (OFP , $\mu\text{g min}^{-1}$) was calculated by the following equation (Atkinson
175 and Arey, 2003),

$$176 \quad \text{OFP} = \sum[\text{HC}_i] \times \text{MIR}_i \quad (2)$$

177 Where $[\text{HC}_i]$ is the emission rate of precursor i ($\mu\text{g min}^{-1}$) with maximum incremental reactivity
178 (MIR) of MIR_i . The MIR could be found in Table S3 and calculation procedures could be found
179 inside the FOQAT packages developed by Tianshu Chen (<https://github.com/tianshu129/foqat>).

180 SOA ($\mu\text{g min}^{-1}$) was estimated by the following equation, where $[\text{HC}_i]$ is the emission rate of
181 precursor i ($\mu\text{g min}^{-1}$) with OH reaction rate of $k_{\text{OH},i}$, ($\text{cm}^3 \cdot \text{molecules}^{-1} \cdot \text{s}^{-1}$) and SOA yield of Y_i
182 (Table S3). The SOA yields of precursors were from literature (Algrim and Ziemann, 2016, 2019;
183 Chan et al., 2009, 2010; Harvey and Petrucci, 2015; Li et al., 2016; Liu et al., 2018; Loza et al., 2014;
184 Matsunaga et al., 2009; McDonald et al., 2018; Shah et al., 2020; Tkacik et al., 2012; Wu et al., 2017)
185 or surrogates from *n*-alkanes in the same volatility bins (Zhao et al., 2014, 2017). The SOA yields
186 utilized in this work are under high NO_x conditions which are underestimation of SOA due to the

187 lower yields compared to low NO_x conditions. $[OH] \times \Delta t$ is the OH exposure and was set to be 14.4
188 $\times 10^{10}$ molecules·cm⁻³·s (~ 1.1 days in OH concentration of 1.5×10^6 molecules·cm⁻³) in order to keep
189 pace with our previous work (Zhang et al., 2021b; Zhu et al., 2021).

$$190 \quad SOA = \sum[HC_i] \times (1 - e^{-k_{OH,i} \times [OH] \times \Delta t}) \times Y_i \quad (3)$$

191 **2.3 Pixel-based analysis to demonstrate the main influencing factor of cooking emissions**

192 Pixel-based analysis was widely used as a dimension reduction tool for data interpretation
193 (Furbo et al., 2014). Pixel-based approaches have been proved to be powerful techniques for the
194 identification of atmospheric gaseous fingerprints (Song et al., 2022). In this work, pixel-based
195 partial least squares-discriminant analysis (PLS-DA) and multiway principal component analysis
196 (MPCA) were utilized for sample classification and key components identification, following the
197 pipeline of RGC×GC toolbox (Quiroz-Moreno et al., 2020). Chromatograms were imported from the
198 network common data form (netCDF). Smoothing, baseline correction, alignment, and
199 chromatogram unfolding were then conducted. MPCA was calculated inside the R language, while
200 PLS-DA was conducted by the interface of RGC×GC and mixOmics packages (González et al., 2012;
201 Lê Cao et al., 2009; Rohart et al., 2017). See more information about the data processing procedure
202 elsewhere (Quiroz-Moreno et al., 2020; Song et al., 2022).

203 PLS-DA is a supervised method for the classification of grouped data. The main influencing
204 factor could be apportioned if one separation result of PLS-DA is much better than the other. MPCA
205 composes matrix $X_{(i,j)}$ into score (S) and loading (L) matrices. Pixel-based MPCA could identify the
206 similarities by resolving chemicals from the positive loading chromatogram (Song et al., 2022).

207 All data processing was accomplished by GC Image® (GC×GC Software, 2.8r2, USA) and R
208 4.1.0 (Chen, 2021; Patil, 2021; R Core Team, 2020).

209 **3 Results and discussions**

210 **3.1 Molecular compositions of S/IVOCs, OFP, and SOA estimation from different dish fumes**

211 Typical chromatograms of four dish emissions are displayed in Figure S3. Chemicals identified
212 are colored in groups in Figure 1. The total mass concentrations of four dishes are displayed in
213 Figure 2. The emission rate of Kung Pao chicken was the highest ($6918 \pm 5924 \mu\text{g min}^{-1}$), followed
214 by fried chicken ($4827 \pm 3308 \mu\text{g min}^{-1}$), pan-fried tofu ($3854 \pm 3809 \mu\text{g min}^{-1}$), and stir-fried

215 cabbage ($697 \pm 548 \mu\text{g min}^{-1}$). Stir-frying procedures of Kung Pao chicken were rather intense,
216 followed by deep-frying chicken. Research has revealed that VOC emissions from quick- and stir-
217 frying or deep-frying cooking methods are much higher (Chen et al., 2018; Ciccone et al., 2020;
218 Kabir and Kim, 2011; Lu et al., 2021).

219 The compositions of the gaseous emissions are exhibited in Figure S4. Aromatics contributed
220 59.1%, 23.6%, 8.1%, and 11.8% of the total mass concentration of Kung Pao chicken, fried chicken,
221 pan-fried tofu, and stir-fried cabbage, while oxygenated compounds accounted for 17.1%, 53.7%,
222 76.9%, and 25.0% of the total concentration, respectively. The compositions of organic in this study
223 diverged from proton transfer reaction mass spectrometer (PTR-MS) measurements (Klein et al.,
224 2016a; Liu et al., 2018), in which aldehydes dominated the emission profiles ($\sim 60\%$). The
225 proportion of aromatics was also different from online Vocus-PTR-ToF measurements in a recent
226 study (Yu et al., 2022). However, the contribution of aromatics was close to a recent study conducted
227 at Chinese restaurants using GC-MS analysis (Huang et al., 2020). The different instruments
228 resulting in different VOC detection ranges could be the explanation for the different patterns. GC \times
229 GC-MS is powerful in resolving complex mixtures with carbon numbers of more than 6. The
230 structural chromatograms and detailed mass spectrum information provide a convincing result in
231 chemical identification (An et al., 2021). In contrast, PTR-MS could detect much more short-chain
232 alkenes and aldehydes with carbon numbers less than 4. However, the isomers of PTR-MS could not
233 be distinguished. Alkanes and some long-chain compounds could not be detected by PTR-MS. For
234 instance, the maximum carbon number of pollutants in Yu et al is 16 ($\text{C}_{16}\text{H}_{26}$) (Yu et al., 2022) while
235 the maximum carbon number of pollutants detected in this work is 30 ($\text{C}_{30}\text{H}_{62}$). $\text{C}_2\text{H}_6\text{O}$, C_4H_8 ,
236 $\text{C}_4\text{H}_8\text{O}_2$, and C_5H_8 were the top species measured by Vocus-PTR-ToF (Yu et al., 2022), which is out
237 of range of our measurement. Compositions of organic emissions diverged significantly and showed
238 a great influence pattern of cooking styles (Wang et al., 2020). Dishes cooked by intense cooking
239 methods, like stir-frying, released more aromatics. Despite this, researches have indicated that the
240 emission patterns of different cooking styles are heavily driven by the thin or thick layer of oil (oil
241 amount), oil temperature, evaporation of water during cooking, and chemical reactions, such as
242 starch gelatinization, and protein denaturation (Atamaleki et al., 2021; Zhang et al., 2020). As for

243 chemical species, toluene, hexanoic acid, and pentanoic acid were extensively detected among meat-
244 related cooking fumes, which were among the top 5 species and accounted for more than half of the
245 total emission rate. A vegetable-related pattern was observed in the emissions of stir-fried cabbage.
246 Alkanes (C10 – C12), alcohols (linalool, butanol), and pinenes (beta-pinene) were the dominant
247 chemical classes. As much as 26.3% and 26.1% of the total organics of stir-fried cabbage emission
248 were alkanes and alkenes (especially pinenes). The high plant wax content (Zhao et al., 2007a) in this
249 dish dramatically influenced the composition of the fume.

250 Although the profiles of compositions diverged from dish to dish, their volatility-polarity
251 patterns remained similar, showing a consistent pattern with a recent study (Yu et al., 2022). The
252 volatility-polarity distributions of the gaseous emissions are displayed in Figure 3. VOCs (B11 and
253 before, saturated vapor concentration $> 10^6 \mu\text{g m}^{-3}$) with low polarity (P1 – P4) dominated the
254 emissions of gas-phase contaminants. Chemicals in the VOC range accounted for 88.7%, 95.6%,
255 85.2%, and 81.4% of the total emission rates of fried chicken, Kung Pao chicken, pan-fried tofu, and
256 stir-fried cabbage emissions, while S/IVOCs accounted for 11.3%, 4.4%, 14.8%, and 18.2%,
257 respectively. However, considering the chemical compositions in each volatility bin, the emission
258 patterns are quite distinct (Figure S5). Oxygenated compounds were widely detected before B13
259 (VOC-IVOC range) in emissions of fried chicken and pan-fried tofu, while aromatics were
260 extensively detected in the B8 range of Kung Pao chicken fumes. Alkanes and alkenes in the B10
261 range dominated the emissions of stir-fried cabbage. From the discussion above, the volatility
262 distribution of cooking emissions obtained from the one-dimensional GC-MS analysis faces large
263 uncertainty in SOA estimation if the polarity is not taken into account. Meanwhile, the volatility-
264 polarity distribution should be equipped with detailed chemical parameters in each bin to precisely
265 estimate SOA.

266 The total emission rates, compositions, and volatility-polarity distributions of OFP and SOA
267 estimation by gaseous precursors are displayed in Figure 2, Figure S4, and Figure 3, respectively.
268 The total OFP and SOA estimation are consistent with the emission rate, as Kung Pao chicken
269 emitted the most pollutants and produced the most ozone formation ($21125 \pm 19447 \mu\text{g min}^{-1}$) and
270 SOA formation ($584 \pm 482 \mu\text{g min}^{-1}$). Pan-fried tofu emitted a little bit less than fried chicken, yet

271 produced more SOA estimation due to a large proportion of short-chain acids (hexanoic acid) (Alves
272 and Pio, 2005; Forstner et al., 1997; Kamens et al., 1999). Short-chain acids are likely derived from
273 scission reactions of allylic hydroperoxides originating from unsaturated fatty acids (Chow, 2007;
274 Goicoechea and Guillén, 2014). Although chemicals in the VOC range dominated ozone and SOA
275 formation, an increase in ozone formation contribution and a decrease in SOA formation contribution
276 compared with the mass proportion of VOCs in EFs were observed. VOCs contributed 90.3% - 99.8%
277 of the ozone estimation, and 68.0% - 89.8% of the total SOA estimation, compared with 81.4% -
278 95.6% in EFs. S/IVOCs explained 10.2% - 32.0% of the SOA estimation. Aromatics (toluene) and
279 alkenes (heptene) were dominant ozone formation precursors in meat-relating dishes (fried chicken,
280 Kung Pao chicken, and pan-fried tofu), while alcohols (butanol and linalool) were predominant for
281 stir-fried cabbage (Atamaleki et al., 2021). Acids (hexanoic acid), aromatics (toluene), alkenes
282 (pinenes), and alkanes were important SOA precursors. We also want to emphasize that there are
283 large uncertainties in SOA estimation. Yu et al measured gas-phase VOC, IVOC, and SVOC
284 precursors by Vocus-PTR-ToF and compared the results with SOA measured from the aerosol mass
285 spectrometer (AMS). 19 ~ 55% of the SOA could be explained. Among them, the SOA estimation
286 from precursors emitted from Kung Pao chicken is the largest even though the SOA mass is the
287 lowest among the four dishes (Yu et al., 2022). The SOA estimation in this work is also the largest
288 regarding Kung Pao chicken emissions. Aromatics and alkenes in Kung Pao chicken fumes
289 contributed 63.6% of the SOA estimation, and the top SOA contributor in Yu et al. were
290 sesquiterpenes and aromatics, showing a consistent pattern between these two studies. It should be
291 noticed that more than 45% of the SOA could not be explained (Yu et al., 2022) and more
292 investigations should be carried on to further identify the emission and evolution of cooking fumes in
293 the atmosphere.

294 **3.2 Molecular compositions of S/IVOCs, OFP, and SOA estimation from fried chicken fumes** 295 **using four types of oils**

296 Typical chromatograms of fried chicken emissions cooked with corn, peanut, soybean, and
297 sunflower oils are displayed in Figure S6. Chemicals identified are colored in groups in Figure S7.
298 Total chemical emission rates were $4827 \pm 3308 \mu\text{g min}^{-1}$, $3423 \pm 988 \mu\text{g min}^{-1}$, $3625 \pm 1834 \mu\text{g min}^{-1}$

299 ¹, and 2268 $\mu\text{g min}^{-1}$ ($n = 1$) for chicken fried with corn, peanut, soybean, and sunflower oils,
300 respectively (Figure 4). Chicken fried with corn oil emitted the most abundant gaseous contaminants.
301 The emission patterns in this work diverged from heated oil fumes (Liu et al., 2018) as in their work
302 heated sunflower oil and peanut oil emitted more organics. Compositions and volatility-polarity
303 distributions of contaminants are displayed in Figure S8 and Figure S9, respectively. Aromatic
304 contributed 23.6%, 20.1%, 50.5%, and 19.8% of the total ERs of fried chicken fumes cooked with
305 corn, peanut, soybean, and sunflower, oils, respectively. Fried chicken fumes cooked with soybean
306 oil were especially abundant in toluene (rank 1st). In the TD-GC \times GC-MS analysis of soybean oil
307 (Figure S10), unsaturated fatty acids (linoleic acid) contributed 31.5% of the total percent response
308 (50.5% aromatics), compared to 10.1% of the total response in corn oil (15.5% aromatics). As a
309 result, the aromatic concentrations and compositions of the fried chicken fumes diverged according
310 to the content of unsaturated fatty acids in the oil (Chow, 2007; Zhang et al., 2019). Butanol was the
311 most abundant chemical when peanut and sunflower oils were used for frying. A previous study
312 indicated that benzene, toluene, and ethylbenzene were the three dominant aromatics in kitchens
313 (Huang et al., 2011; Yi et al., 2019). Monocyclic aromatics are formed from linoleic and linolenic
314 acyl groups in the oil (Atamaleki et al., 2021; Uriarte and Guillén, 2010). The decomposition of
315 linoleic and linolenic acid forms alkadienals and then form aromatics once lose H₂O (Atamaleki et
316 al., 2021; Zhang et al., 2019). According to previous studies, soybean oil contains more unsaturated
317 fatty acids, especially linolenic acid (Kostik et al., 2013; Ryan et al., 2008). Oxygenated compounds
318 were extensively detected, which accounted for 53.7%, 33.1%, 24.7%, and 35.0% of the total ERs
319 (Figure S8). Short-chain acids and aldehydes were the most abundant oxygenated compounds and
320 were dominated by hexanoic acid, hexanal, and nonanal. Despite acids and aldehydes, alcohols
321 (butanol, octenal) were heavily detected in the fume of corn oil-fried chicken, which was also
322 supported by another study (Liu et al., 2018; Reyes-Villegas et al., 2018). The short-chain
323 contaminants were fundamentally formed by hydroperoxide decomposition (originated from oleate
324 and linoleate in the oil) through homolytic scission or homolytic β -scission reactions (Chow, 2007;
325 Goicoechea and Guillén, 2014) and quickly evaporated from the oil. Either aromatics or oxygenated
326 compounds detected in the gas phase showed high sensitivity to oil compositions, especially

327 potentially influenced by oleic and linoleic compounds.

328 Although pollutants were dominated by aromatics, alkanes, and oxygenated compounds with
329 volatility bins of B9 to B12 (VOC-IVOC range, saturated vapor concentration $> 10^6 \mu\text{g m}^{-3}$) and
330 polarity bins of P1 to P5 (low to medium polarity), significant diversities of volatility-polarity
331 distributions were observed (Figure S9). The chemical compositions in each volatility bin were also
332 distinct (Figure S11). IVOCs accounted for as much as 22.8% and 23.7% of the total ERs when
333 peanut and sunflower oils were utilized for frying (Kostik et al., 2013; Ryan et al., 2008). The peanut
334 oil was much more abundant in oleic acid (41.5%), while the proportion of linoleic acid in sunflower
335 is 36.6% (Figure S10). The proportion of unsaturated acids in peanut and sunflower oils is higher
336 than that of other oils.

337 Chicken fried in soybean oil produced the highest OFP ($10134 \pm 5958 \mu\text{g min}^{-1}$) while chicken
338 fried in corn oil resulted in the most SOA estimation ($426 \pm 270 \mu\text{g min}^{-1}$). Aromatics were
339 predominant in ozone formation, while oxygenated compounds, alkenes, alkanes, and aromatics
340 were important SOA precursors. S/IVOCs were non-negligible SOA precursors because they
341 contributed as much as 22.0%, 28.2%, 24.0%, and 29.7% of the SOA estimation. Without S/IVOCs,
342 a large proportion of SOA would be underestimated. Our work illustrated the importance of the
343 measurement of S/IVOC precursors which was absent in previous studies (Liu et al., 2018; Zhang et
344 al., 2021b). Despite the importance of aldehydes revealed in previous studies (Klein et al., 2016a;
345 Liu et al., 2018), our results demonstrated that alkanes, pinenes, and short-chain acids are also key
346 precursors in cooking SOA production (Huang et al., 2020).

347 **3.3 Elucidating the influencing factor and inferring in-oil reactions of cooking emissions**

348 From the discussion above, cooking style and oil could influence emissions dramatically. But
349 we still wonder what is the main predominant factor shaping the profile of cooking emission. In
350 other words, we want to learn whether the cooking styles affect cooking patterns more. A pixel-based
351 partial least squares-discriminant analysis (PLS-DA) was utilized to investigate the key factor. The
352 results are displayed in Figure 5. PLS-DA is a supervised classification method requiring the data
353 pre-grouping. The separation results of the PLS-DA indicate the crucial pattern behind the
354 classification. When oil was set as the grouping variable, the separation was much better than setting

355 the dish as the grouping variable (Figure 5 (a) and (b)). The separation results demonstrated that the
356 oil used during the cooking procedure is much more crucial in shaping the emission profiles than the
357 cooking style. The variance of cooking fumes could be largely explained by the different oil utilized.

358 Plenty of physical and chemical reactions occur during the cooking procedure (Chow, 2007;
359 Goicoechea and Guillén, 2014). To demonstrate the direct effect of oil on cooking emissions, PLS-
360 DA and MPCA analyses were utilized. The PLS-DA result showed that cooking emissions diverged
361 from oils (Figure 5 (c)), indicating that the physical reactions (evaporation of edible oils) were not
362 the main reactions during the cooking procedure. MPCA results showed the chromatogram
363 similarities (positive loading) of oils and emissions (Figure 5(d)). Fatty acids (palmitic acid, oleic
364 acid, and linoleic acid), decanal, and decadienals were the key fingerprints. The pattern is linked to
365 the autooxidation procedure of oil. Oil autooxidation is a three-step free radical process: initiation,
366 propagation, and termination (Atamaleki et al., 2021; Uriarte and Guillén, 2010; Yi et al., 2019). The
367 key initiation step is the formation of lipid radical ($R\bullet$) from unsaturated fatty acid (RH). $R\bullet$ then
368 reacts with O_2 to form peroxy radical ($ROO\bullet$) and then form hydroperoxides (ROOH). Another RH
369 changes to $R\bullet$ in this propagation process. During the termination process, the decomposition of
370 ROOH forms monomeric (keto-, hydroxy-, and epoxy- derivatives), polymeric (RR, ROR, ROOR),
371 and volatile compounds (short-chain acids, aldehydes, alcohols, ketones). In more detail, the
372 oxidation of unsaturated fatty acids (such as linoleic acid) in oil leads to the production of
373 alkadienals (such as (*E, E*)-2,4-decadienal) which form aromatics (butylbenzene) by losing H_2O
374 (Atamaleki et al., 2021; Zhang et al., 2019). This is consistent with the analysis of edible oils in this
375 work. Corn oil contained a less amount of unsaturated fatty acids (Figure S10), and the emission of
376 aromatics cooked with coil oil was the lowest among the 4 types of oils used. The emission pattern is
377 in line with previous studies (Atamaleki et al., 2021). The short-chain aldehydes and acids are
378 derived from scission reactions of allylic hydroperoxides originated from unsaturated fatty acids
379 (Chow, 2007; Goicoechea and Guillén, 2014), while the dehydration reaction of alkenals forms
380 furanones (Zhang et al., 2019). Aldehydes, acids, and furanones are regarded as potential tracers of
381 cooking emissions (Klein et al., 2016a; Wang et al., 2020; Zeng et al., 2020) and were widely
382 detected in this work. These highly volatile contaminants escape from oil immediately and lead to an

383 accumulation of oxygenated compounds in the gas phase. Figure S12 shows the inferred reactions
384 originating from linoleic acid and oleic acid. The significant correlations ($p < 0.1$) between key
385 components (Figure S13) further support the chemical reactions demonstrated in Figure S12. The
386 key chemicals elucidated by the MPCA analysis (Figure 5 (d)) illustrated that the cooking emissions
387 are largely driven by the autooxidation of oil, which is accelerated during the heating and cooking
388 procedures (Atamaleki et al., 2021; Uriarte and Guillén, 2010; Yi et al., 2019; Zhang et al., 2019).

389 **4 Atmospheric Implications**

390 In this work, gaseous VOCs, IVOCs, and SVOCs from cooking fumes are quantified in detail.
391 The influence of cooking style and oil is taken into account in this work. S/IVOC species are key
392 components as they contributed 10.2% - 32.0% of the total SOA estimation. Previous works might
393 underestimate the importance of cooking fumes to SOA formation because only a series of IVOC
394 homologs were quantified (Liu et al., 2018). For instance, aldehydes only accounted for 0.7% -10.1%
395 of the total SOA estimation. If only aldehydes are taken into consideration, SOA will be
396 underestimated 9.9 ~ 139 times. We still need to stress that although GC×GC is utilized, UCMs still
397 occur sharing a proportion of 5% of the total response in this work. Acids and aldehydes tail in the
398 second column and cause uncertainties in the quantification procedure. Meanwhile, TD-GC×GC-MS
399 does not comprehensively measure all compounds. Acids can decompose during thermal desorption
400 if no derivatization was performed. Meanwhile, the decomposition of SVOC compounds could
401 produce small molecules in the VOC or IVOC range. The TD process could introduce
402 underestimation for SVOC compounds while causing overestimations of VOC and IVOC species.
403 Highly polar compounds do not elute from the GC column. This may lead to biases in estimating
404 volatility and polarity distributions. Comparisons between GC×GC and chemical ionization mass
405 spectrometers (CIMS) should be further implemented to give a full glimpse of cooking organic
406 compounds.

407 We also first proposed a novel two-dimensional panel elucidating the physiochemical properties
408 of contaminants from the perspectives of their volatilities and polarities. This novel scheme is
409 appropriate to demonstrate the complicated evolution of contaminants clearly and provide new
410 insight into the previously 1D-bins method. The volatility-polarity panel inherited the spirit of the

411 two-dimensional volatility-based set (2D-VBS) (Donahue et al., 2011, 2012) and would be further
412 implemented in the analysis of complex ambient or source samples along with the powerful
413 separating capacity of GC×GC. We would like to emphasize the importance of combining the
414 volatility-polarity distribution with detailed chemical information for a precise estimation of SOA.

415 We also provide powerful tools in speciating the main driving factor and inferring chemical
416 reactions in rather complicated systems. The pixel-based PLS-DA and MPCA analysis greatly
417 enhance our learning of complex chromatograms and provide us with new insight into the dimension
418 reduction processes. The analyzing scheme could benefit those analysts with less experience in
419 GC×GC data processing.

420 Our results demonstrated that both cooking styles (dish) and oils influence the cooking
421 emissions. Kung Pao chicken emitted more pollutants than other dishes due to its rather intense
422 cooking method. Cooking materials could also influence the compositions of fumes as well.
423 Aromatics and oxygenated compounds were extensively detected among meat-related cooking fumes,
424 while a vegetable-related pattern was observed in the emissions of stir-fried cabbage. As much as
425 22.2% and 29.5% of the total organics of stir-fried cabbage emission were alkanes and alkenes
426 (especially pinenes). On the other hand, oils greatly influence the composition and volatility-polarity
427 distribution of pollutants. Chicken fried with corn oil emitted the most abundant contaminants.
428 However, the ozone formation from soybean-oil fried chicken fumes was much higher. Considering
429 the high consumption proportion of soybean oil (~ 44% in volume of oil usage) in China (Jamet and
430 Chaumet, 2016), the influence of using soybean cooking oil on ozone formation might be
431 underestimated. The MPCA results also indicate that the heating and cooking procedure greatly
432 enhances the autooxidation of oil. MPCA results emphasize the importance of the unsaturated fatty
433 acid-alkadienal-volatile product mechanism. More studies need to be carried on to elucidate the key
434 chemical reactions between the food and oil.

435

436 **Acknowledgment**

437 The work was funded by National Natural Science Foundation of China (No. 41977179,
438 91844301), the special fund of State Key Joint Laboratory of Environment Simulation and Pollution

439 Control (No. 22Y01SSPCP), the Open Research Fund of State Key Laboratory of Multi-phase
440 Complex Systems (No. MPCS-2021-D-12). We greatly thank Mengxue Tong for the sample
441 collection.

442

443 **Credit Author Statement:**

444 Kai Song, Yuanzheng Gong, and Daqi Lv conducted the experiments.

445 Kai Song and Yuanzheng Gong analyzed the data.

446 Kai Song, Song Guo, Yuanzheng Gong, Daqi Lv, Yuan Zhang, Zichao Wan, Tianyu Li, Wenfei Zhu,
447 Hui Wang, Ying Yu, Rui Tan, Ruizhe Shen, Sihua Lu, Shuangde Li, Yunfa Chen, and Min Hu
448 discussed the scientific results and review the paper.

449 Kai Song and Song Guo wrote the paper.

450

451 **Reference**

452 Abdel-Shafy, H. I. and Mansour, M. S. M.: A review on polycyclic aromatic hydrocarbons: Source,
453 environmental impact, effect on human health and remediation, *Egypt. J. Pet.*, 25(1), 107–123,
454 doi:10.1016/J.EJPE.2015.03.011, 2016.

455 Abdullahi, K. L., Delgado-Saborit, J. M. and Harrison, R. M.: Emissions and indoor concentrations
456 of particulate matter and its specific chemical components from cooking: A review., 2013.

457 Algrim, L. B. and Ziemann, P. J.: Effect of the Keto Group on Yields and Composition of Organic
458 Aerosol Formed from OH Radical-Initiated Reactions of Ketones in the Presence of NO_x, *J. Phys.*
459 *Chem. A*, 120(35), 6978–6989, doi:10.1021/acs.jpca.6b05839, 2016.

460 Algrim, L. B. and Ziemann, P. J.: Effect of the Hydroxyl Group on Yields and Composition of
461 Organic Aerosol Formed from OH Radical-Initiated Reactions of Alcohols in the Presence of NO_x,
462 *ACS Earth Sp. Chem.*, 3(3), 413–423, doi:10.1021/acsearthspacechem.9b00015, 2019.

463 Alves, C., Vicente, A., Pio, C., Kiss, G., Hoffer, A., Decesari, S., Prevôt, A. S. H., Minguillón, M. C.,
464 Querol, X., Hillamo, R., Spindler, G. and Swietlicki, E.: Organic compounds in aerosols from
465 selected European sites - Biogenic versus anthropogenic sources, *Atmos. Environ.*, 59, 243–255,
466 doi:10.1016/J.ATMOSENV.2012.06.013, 2012.

467 Alves, C. A. and Pio, C. A.: Secondary organic compounds in atmospheric aerosols: Speciation and
468 formation mechanisms, *J. Braz. Chem. Soc.*, 16(5), 1017–1029, doi:10.1590/s0103-
469 50532005000600020, 2005.

470 Alves, C. A., Vicente, E. D., Evtyugina, M., Vicente, A. M. P., Sainnokhoi, T. A. and Kováts, N.:
471 Cooking activities in a domestic kitchen: Chemical and toxicological profiling of emissions, *Sci.*
472 *Total Environ.*, 772, 145412, doi:10.1016/j.scitotenv.2021.145412, 2021.

473 Amouei Torkmahalleh, M., Gorjinezhad, S., Unluevcek, H. S. and Hopke, P. K.: Review of factors
474 impacting emission/concentration of cooking generated particulate matter, , 586, 1046–1056,
475 doi:10.1016/J.SCITOTENV.2017.02.088, 2017.

476 An, Z., Li, X., Shi, Z., Williams, B. J., Harrison, R. M. and Jiang, J.: Frontier review on
477 comprehensive two-dimensional gas chromatography for measuring organic aerosol, *J. Hazard.*
478 *Mater. Lett.*, 2, 100013, doi:10.1016/j.hazl.2021.100013, 2021.

479 Atamaleki, A., Motesaddi Zarandi, S., Massoudinejad, M., Samimi, K., Fakhri, Y., Ghorbanian, M.
480 and Mousavi Khaneghah, A.: The effect of frying process on the emission of the volatile organic
481 compounds and monocyclic aromatic group (BTEX), *Int. J. Environ. Anal. Chem.*, 1–14,
482 doi:10.1080/03067319.2021.1950148, 2021.

483 Atkinson, R. and Arey, J.: Atmospheric Degradation of Volatile Organic Compounds, *Chem. Rev.*,
484 103(12), 4605–4638, doi:10.1021/cr0206420, 2003.

485 Awogbemi, O., Onuh, E. I. and Inambao, F. L.: Comparative study of properties and fatty acid
486 composition of some neat vegetable oils and waste cooking oils, *Int. J. Low-Carbon Technol.*, 14(3),
487 417–425, doi:10.1093/ijlct/ctz038, 2019.

488 Bruns, E. A., El Haddad, I., Slowik, J. G., Kilic, D., Klein, F., Baltensperger, U. and Prévôt, A. S. H.:
489 Identification of significant precursor gases of secondary organic aerosols from residential wood
490 combustion, *Sci. Rep.*, 6, doi:10.1038/srep27881, 2016.

491 Chan, A. W. H., Kautzman, K. E., Chhabra, P. S., Surratt, J. D., Chan, M. N., Crouse, J. D., Kürten,
492 A., Wennberg, P. O., Flagan, R. C. and Seinfeld, J. H.: Secondary organic aerosol formation from
493 photooxidation of naphthalene and alkylnaphthalenes: Implications for oxidation of intermediate
494 volatility organic compounds (IVOCs), *Atmos. Chem. Phys.*, 9(9), 3049–3060, doi:10.5194/acp-9-

495 3049-2009, 2009.

496 Chan, A. W. H., Chan, M. N., Surratt, J. D., Chhabra, P. S., Loza, C. L., Crounse, J. D., Yee, L. D.,
497 Flagan, R. C., Wennberg, P. O. and Seinfeld, J. H.: Role of aldehyde chemistry and NO_x
498 concentrations in secondary organic aerosol formation, *Atmos. Chem. Phys.*, 10(15), 7169–7188,
499 doi:10.5194/ACP-10-7169-2010, 2010.

500 Chen, C., Zhao, Y. and Zhao, B.: Emission Rates of Multiple Air Pollutants Generated from Chinese
501 Residential Cooking, *Environ. Sci. Technol.*, 52(3), 1081–1087, doi:10.1021/acs.est.7b05600, 2018.

502 Chen, C. Y., Kuo, Y. C., Wang, S. M., Wu, K. R., Chen, Y. C. and Tsai, P. J.: Techniques for
503 predicting exposures to polycyclic aromatic hydrocarbons (PAHs) emitted from cooking processes
504 for cooking workers, *Aerosol Air Qual. Res.*, 19(2), 307–317, doi:10.4209/aaqr.2018.09.0346, 2019.

505 Chen, T.: foqat: Field Observation Quick Analysis Toolkit, [online] Available from:
506 <https://doi.org/10.5281/zenodo.4735828>, 2021.

507 Chow, C. K.: Fatty acids in foods and their health implications, third edition., 2007.

508 Ciccone, M., Chambers, D., Chambers, E. and Talavera, M.: Determining which cooking method
509 provides the best sensory differentiation of potatoes, *Foods*, 9(4), doi:10.3390/foods9040451, 2020.

510 Cordero, C., Schmarr, H. G., Reichenbach, S. E. and Bicchi, C.: Current Developments in Analyzing
511 Food Volatiles by Multidimensional Gas Chromatographic Techniques, *J. Agric. Food Chem.*,
512 66(10), 2226–2236, doi:10.1021/acs.jafc.6b04997, 2018.

513 Donahue, N. M., Epstein, S. A., Pandis, S. N. and Robinson, A. L.: A two-dimensional volatility
514 basis set: 1. organic-aerosol mixing thermodynamics, *Atmos. Chem. Phys.*, 11(7), 3303–3318,
515 doi:10.5194/acp-11-3303-2011, 2011.

516 Donahue, N. M., Kroll, J. H., Pandis, S. N. and Robinson, A. L.: A two-dimensional volatility basis
517 set-Part 2: Diagnostics of organic-aerosol evolution, *Atmos. Chem. Phys.*, 12(2), 615–634,
518 doi:10.5194/acp-12-615-2012, 2012.

519 Forstner, H. J. L., Flagan, R. C. and Seinfeld, J. H.: Molecular speciation of secondary organic
520 aerosol from photooxidation of the higher alkenes: 1-octene and 1-decene, *Atmos. Environ.*, 31(13),
521 1953–1964, doi:10.1016/S1352-2310(96)00356-1, 1997.

522 Fullana, A., Carbonell-Barrachina, A. A. and Sidhu, S.: Comparison of volatile aldehydes present in

523 the cooking fumes of extra virgin olive, olive, and canola oils, *J. Agric. Food Chem.*, 52(16), 5207–
524 5214, doi:10.1021/JF035241F, 2004.

525 Furbo, S., Hansen, A. B., Skov, T. and Christensen, J. H.: Pixel-based analysis of comprehensive
526 two-dimensional gas chromatograms (color plots) of petroleum: A tutorial, *Anal. Chem.*, 86(15),
527 7160–7170, doi:10.1021/ac403650d, 2014.

528 Gligorovski, S., Li, X. and Herrmann, H.: Indoor (Photo)chemistry in China and Resulting Health
529 Effects, *Environ. Sci. Technol.*, 52(19), 10909–10910, doi:10.1021/acs.est.8b04739, 2018.

530 Goicoechea, E. and Guillén, M. D.: Volatile compounds generated in corn oil stored at room
531 temperature. Presence of toxic compounds, *Eur. J. Lipid Sci. Technol.*, 116(4), 395–406,
532 doi:10.1002/ejlt.201300244, 2014.

533 González, I., Cao, K. A. L., Davis, M. J. and Déjean, S.: Visualising associations between paired
534 “omics” data sets, *BioData Min.*, 5(1), doi:10.1186/1756-0381-5-19, 2012.

535 Guo, S., Hu, M., Guo, Q., Zhang, X., Zheng, M., Zheng, J., Chang, C. C., Schauer, J. J. and Zhang,
536 R.: Primary sources and secondary formation of organic aerosols in Beijing, China, *Environ. Sci.*
537 *Technol.*, 46(18), 9846–9853, doi:10.1021/es2042564, 2012.

538 Guo, S., Hu, M., Zamora, M. L., Peng, J., Shang, D., Zheng, J., Du, Z., Wu, Z., Shao, M., Zeng, L.,
539 Molina, M. J. and Zhang, R.: Elucidating severe urban haze formation in China, *Proc. Natl. Acad.*
540 *Sci. U. S. A.*, 111(49), 17373–17378, doi:10.1073/pnas.1419604111, 2014.

541 Guo, S., Hu, M., Peng, J., Wu, Z., Zamora, M. L., Shang, D., Du, Z., Zheng, J., Fang, X., Tang, R.,
542 Wu, Y., Zeng, L., Shuai, S., Zhang, W., Wang, Y., Ji, Y., Li, Y., Zhang, A. L., Wang, W., Zhang, F.,
543 Zhao, J., Gong, X., Wang, C., Molina, M. J. and Zhang, R.: Remarkable nucleation and growth of
544 ultrafine particles from vehicular exhaust, *Proc. Natl. Acad. Sci. U. S. A.*, 117(7), 3427–3432,
545 doi:10.1073/pnas.1916366117, 2020.

546 Gysel, N., Dixit, P., Schmitz, D. A., Engling, G., Cho, A. K., Cocker, D. R. and Karavalakis, G.:
547 Chemical speciation, including polycyclic aromatic hydrocarbons (PAHs), and toxicity of particles
548 emitted from meat cooking operations, *Sci. Total Environ.*, 633, 1429–1436,
549 doi:10.1016/j.scitotenv.2018.03.318, 2018.

550 Harvey, R. M. and Petrucci, G. A.: Control of ozonolysis kinetics and aerosol yield by nuances in the

551 molecular structure of volatile organic compounds, *Atmos. Environ.*, 122, 188–195,
552 doi:10.1016/j.atmosenv.2015.09.038, 2015.

553 He, L. Y., Hu, M., Wang, L., Huang, X. F. and Zhang, Y. H.: Characterization of fine organic
554 particulate matter from Chinese cooking, *J. Environ. Sci.*, 16(4), 570–575, 2004.

555 Hu, M., Guo, S., Peng, J. F. and Wu, Z. J.: Insight into characteristics and sources of PM_{2.5} in the
556 Beijing-Tianjin-Hebei region, China, *Natl. Sci. Rev.*, 2(3), 257–258, doi:10.1093/nsr/nwv003, 2015.

557 Huang, X., Han, D., Cheng, J., Chen, X., Zhou, Y., Liao, H., Dong, W. and Yuan, C.: Characteristics
558 and health risk assessment of volatile organic compounds (VOCs) in restaurants in Shanghai,
559 *Environ. Sci. Pollut. Res.*, 27(1), 490–499, doi:10.1007/s11356-019-06881-6, 2020.

560 Huang, Y., Ho, S. S. H., Ho, K. F., Lee, S. C., Yu, J. Z. and Louie, P. K. K.: Characteristics and
561 health impacts of VOCs and carbonyls associated with residential cooking activities in Hong Kong, *J.*
562 *Hazard. Mater.*, 186(1), 344–351, doi:10.1016/j.jhazmat.2010.11.003, 2011.

563 Huo, Y., Guo, Z., Liu, Y., Wu, D., Ding, X., Zhao, Z., Wu, M., Wang, L., Feng, Y., Chen, Y., Wang,
564 S., Li, Q. and Chen, J.: Addressing Unresolved Complex Mixture of I/SVOCs Emitted From
565 Incomplete Combustion of Solid Fuels by Nontarget Analysis, *J. Geophys. Res. Atmos.*, 126(23),
566 e2021JD035835, doi:10.1029/2021JD035835, 2021.

567 Jamet, J. P. and Chaumet, J. M.: Soybean in China: Adaptating to the liberalization, *OCL - Oilseeds*
568 *fats, Crop. Lipids*, 23(6), doi:10.1051/ocl/2016044, 2016.

569 Kabir, E. and Kim, K. H.: An investigation on hazardous and odorous pollutant emission during
570 cooking activities, *J. Hazard. Mater.*, 188(1–3), 443–454, doi:10.1016/j.jhazmat.2011.01.113, 2011.

571 Kamens, R., Jang, M., Chien, C. J. and Leach, K.: Aerosol formation from the reaction of α -pinene
572 and ozone using a gas- phase kinetics-aerosol partitioning model, *Environ. Sci. Technol.*, 33(9),
573 1430–1438, doi:10.1021/es980725r, 1999.

574 Katragadda, H. R., Fullana, A., Sidhu, S. and Carbonell-Barrachina, Á. A.: Emissions of volatile
575 aldehydes from heated cooking oils, *Food Chem.*, 120(1), 59–65,
576 doi:10.1016/j.foodchem.2009.09.070, 2010.

577 Kim, K. H., Jahan, S. A., Kabir, E. and Brown, R. J. C.: A review of airborne polycyclic aromatic
578 hydrocarbons (PAHs) and their human health effects, Elsevier Ltd., 2013.

579 Klein, F., Platt, S. M., Farren, N. J., Detournay, A., Bruns, E. A., Bozzetti, C., Daellenbach, K. R.,
580 Kilic, D., Kumar, N. K., Pieber, S. M., Slowik, J. G., Temime-Roussel, B., Marchand, N., Hamilton,
581 J. F., Baltensperger, U., Prévôt, A. S. H. H., El Haddad, I., Haddad, I. El and El Haddad, I.:
582 Characterization of Gas-Phase Organics Using Proton Transfer Reaction Time-of-Flight Mass
583 Spectrometry: Cooking Emissions, *Environ. Sci. Technol.*, 50(3), 1243–1250,
584 doi:10.1021/acs.est.5b04618, 2016a.

585 Klein, F., Farren, N. J., Bozzetti, C., Daellenbach, K. R., Kilic, D., Kumar, N. K., Pieber, S. M.,
586 Slowik, J. G., Tuthill, R. N., Hamilton, J. F., Baltensperger, U., Prévôt, A. S. H. and El Haddad, I.:
587 Indoor terpene emissions from cooking with herbs and pepper and their secondary organic aerosol
588 production potential, *Sci. Rep.*, 6, doi:10.1038/srep36623, 2016b.

589 Kostik, V., Memeti, S. and Bauer, B.: Fatty acid composition of edible oils and fats, *J. Hyg. Eng.*
590 *Des.*, 4, 112–116, 2013.

591 Lê Cao, K. A., González, I. and Déjean, S.: IntegrOmics: An R package to unravel relationships
592 between two omics datasets, *Bioinformatics*, 25(21), 2855–2856, doi:10.1093/bioinformatics/btp515,
593 2009.

594 Li, L., Tang, P., Nakao, S. and Cocker, D. R.: Impact of molecular structure on secondary organic
595 aerosol formation from aromatic hydrocarbon photooxidation under low-NO_x conditions, *Atmos.*
596 *Chem. Phys.*, 16(17), 10793–10808, doi:10.5194/acp-16-10793-2016, 2016.

597 Lin, Y., Shao, M. and Lu, S.: The emission characteristics of hydrocarbon from Chinese cooking
598 under smoke control, *Int. J. Environ. Anal. Chem.*, 90(9), 708–721,
599 doi:10.1080/03067310903194964, 2010.

600 Liu, T., Wang, Z., Huang, D. D., Wang, X. and Chan, C. K.: Significant Production of Secondary
601 Organic Aerosol from Emissions of Heated Cooking Oils, *Environ. Sci. Technol. Lett.*, 5(1), 32–37,
602 doi:10.1021/acs.estlett.7b00530, 2018.

603 Loza, C. L., Craven, J. S., Yee, L. D., Coggon, M. M., Schwantes, R. H., Shiraiwa, M., Zhang, X.,
604 Schilling, K. A., Ng, N. L., Canagaratna, M. R., Ziemann, P. J., Flagan, R. C. and Seinfeld, J. H.:
605 Secondary organic aerosol yields of 12-carbon alkanes, *Atmos. Chem. Phys.*, 14(3), 1423–1439,
606 doi:10.5194/acp-14-1423-2014, 2014.

607 Lu, F., Shen, B., Li, S., Liu, L., Zhao, P. and Si, M.: Exposure characteristics and risk assessment of
608 VOCs from Chinese residential cooking, *J. Environ. Manage.*, 289, 112535,
609 doi:10.1016/J.JENVMAN.2021.112535, 2021.

610 Ma, S., Yue, C., Tang, J., Lin, M., Zhuo, M., Yang, Y., Li, G. and An, T.: Occurrence and
611 distribution of typical semi-volatile organic chemicals (SVOCs) in paired indoor and outdoor
612 atmospheric fine particle samples from cities in southern China, *Environ. Pollut.*, 269,
613 doi:10.1016/J.ENVPOL.2020.116123, 2021.

614 Matsunaga, A., Docherty, K. S., Lim, Y. B. and Ziemann, P. J.: Composition and yields of secondary
615 organic aerosol formed from OH radical-initiated reactions of linear alkenes in the presence of NO_x:
616 Modeling and measurements, *Atmos. Environ.*, 43(6), 1349–1357,
617 doi:10.1016/j.atmosenv.2008.12.004, 2009.

618 McDonald, B. C., De Gouw, J. A., Gilman, J. B., Jathar, S. H., Akherati, A., Cappa, C. D., Jimenez,
619 J. L., Lee-Taylor, J., Hayes, P. L., McKeen, S. A., Cui, Y. Y., Kim, S. W., Gentner, D. R., Isaacman-
620 VanWertz, G., Goldstein, A. H., Harley, R. A., Frost, G. J., Roberts, J. M., Ryerson, T. B. and
621 Trainer, M.: Volatile chemical products emerging as largest petrochemical source of urban organic
622 emissions, *Science* (80-.), 359(6377), 760–764, doi:10.1126/science.aaq0524, 2018.

623 Nabi, D. and Arey, J. S.: Predicting Partitioning and Diffusion Properties of Nonpolar Chemicals in
624 Biotic Media and Passive Sampler Phases by GC × GC, *Environ. Sci. Technol.*, 51(5), 3001–3011,
625 doi:10.1021/acs.est.6b05071, 2017.

626 Nabi, D., Gros, J., Dimitriou-Christidis, P. and Arey, J. S.: Mapping environmental partitioning
627 properties of nonpolar complex mixtures by use of GC × GC, *Environ. Sci. Technol.*, 48(12), 6814–
628 6826, doi:10.1021/es501674p, 2014.

629 Patil, I.: Visualizations with statistical details: The “ggstatsplot” approach, *J. Open Source Softw.*,
630 6(61), 3167, doi:10.21105/joss.03167, 2021.

631 Pei, B., Cui, H., Liu, H. and Yan, N.: Chemical characteristics of fine particulate matter emitted from
632 commercial cooking, *Front. Environ. Sci. Eng.*, 10(3), 559–568, doi:10.1007/s11783-016-0829-y,
633 2016.

634 Peng, C. Y., Lan, C. H., Lin, P. C. and Kuo, Y. C.: Effects of cooking method, cooking oil, and food

635 type on aldehyde emissions in cooking oil fumes, *J. Hazard. Mater.*, 324, 160–167,
636 doi:10.1016/j.jhazmat.2016.10.045, 2017.

637 Quiroz-Moreno, C., Furlan, M. F., Belinato, J. R., Augusto, F., Alexandrino, G. L. and Mogollón, N.
638 G. S.: RGCxGC toolbox: An R-package for data processing in comprehensive two-dimensional gas
639 chromatography-mass spectrometry, *Microchem. J.*, 156, 104830, doi:10.1016/j.microc.2020.104830,
640 2020.

641 R Core Team: R Core Team 2020 R: A language and environment for statistical computing. R
642 foundation for statistical computing. <https://www.R-project.org/>, , 2020 [online] Available from:
643 <http://www.r-project.org/>, 2020.

644 Reyes-Villegas, E., Bannan, T., Breton, M. Le, Mehra, A., Priestley, M., Percival, C., Coe, H., Allan,
645 J. D., Le Breton, M., Mehra, A., Priestley, M., Percival, C., Coe, H. and Allan, J. D.: Online
646 Chemical Characterization of Food-Cooking Organic Aerosols: Implications for Source
647 Apportionment, *Environ. Sci. Technol.*, 52(9), 5308–5318, doi:10.1021/acs.est.7b06278, 2018.

648 Rohart, F., Gautier, B., Singh, A. and Lê Cao, K. A.: mixOmics: an R package for ‘omics feature
649 selection and multiple data integration, *bioRxiv*, 13(11), doi:10.1101/108597, 2017.

650 Ryan, L. C., Mestrallet, M. G., Nepote, V., Conci, S. and Grosso, N. R.: Composition, stability and
651 acceptability of different vegetable oils used for frying peanuts, *Int. J. Food Sci. Technol.*, 43(2),
652 193–199, doi:10.1111/j.1365-2621.2006.01288.x, 2008.

653 Schauer, J. J., Kleeman, M. J., Cass, G. R. and Simoneit, B. R. T.: Measurement of emissions from
654 air pollution sources. 1. C1 through C29 organic compounds from meat charbroiling, *Environ. Sci.*
655 *Technol.*, 33(10), 1566–1577, doi:10.1021/es980076j, 1999.

656 Schauer, J. J., Kleeman, M. J., Cass, G. R. and Simoneit, B. R. T.: Measurement of emissions from
657 air pollution sources. 4. C1-C27 organic compounds from cooking with seed oils, *Environ. Sci.*
658 *Technol.*, 36(4), 567–575, doi:10.1021/es002053m, 2002.

659 Shah, R. U., Coggon, M. M., Gkatzelis, G. I., McDonald, B. C., Tasoglou, A., Huber, H., Gilman, J.,
660 Warneke, C., Robinson, A. L. and Presto, A. A.: Urban Oxidation Flow Reactor Measurements
661 Reveal Significant Secondary Organic Aerosol Contributions from Volatile Emissions of Emerging
662 Importance, *Environ. Sci. Technol.*, 54(2), 714–725, doi:10.1021/acs.est.9b06531, 2020.

663 Song, K., Gong, Y., Guo, S., Lv, D., Wang, H., Wan, Z., Yu, Y., Tang, R., Li, T., Tan, R., Zhu, W.,
664 Shen, R. and Lu, S.: Investigation of partition coefficients and fingerprints of atmospheric gas- and
665 particle-phase intermediate volatility and semi-volatile organic compounds using pixel-based
666 approaches, *J. Chromatogr. A*, 1665, 462808, doi:10.1016/j.chroma.2022.462808, 2022.

667 Takhar, M., Li, Y. and W. H. Chan, A.: Characterization of secondary organic aerosol from heated-
668 cooking-oil emissions: Evolution in composition and volatility, *Atmos. Chem. Phys.*, 21(6), 5137–
669 5149, doi:10.5194/ACP-21-5137-2021, 2021.

670 Tang, R., Wu, Z. Z. Z. Z. Z., Li, X., Wang, Y., Shang, D., Xiao, Y., Li, M., Zeng, L., Wu, Z. Z. Z. Z.
671 Z., Hallquist, M., Hu, M. and Guo, S.: Primary and secondary organic aerosols in summer 2016 in
672 Beijing, *Atmos. Chem. Phys.*, 18(6), 4055–4068, doi:10.5194/acp-18-4055-2018, 2018.

673 Tang, R., Lu, Q., Guo, S., Wang, H., Song, K., Yu, Y., Tan, R., Liu, K., Shen, R., Chen, S., Zeng, L.,
674 Jorga, S. D., Zhang, Z., Zhang, W., Shuai, S. and Robinson, A. L.: Measurement report: Distinct
675 emissions and volatility distribution of intermediate-volatility organic compounds from on-road
676 Chinese gasoline vehicles: Implication of high secondary organic aerosol formation potential, *Atmos.*
677 *Chem. Phys.*, 21(4), 2569–2583, doi:10.5194/acp-21-2569-2021, 2021.

678 Tkacik, D. S., Presto, A. A., Donahue, N. M. and Robinson, A. L.: Secondary organic aerosol
679 formation from intermediate-volatility organic compounds: Cyclic, linear, and branched alkanes,
680 *Environ. Sci. Technol.*, 46(16), 8773–8781, doi:10.1021/es301112c, 2012.

681 Uriarte, P. S. and Guillén, M. D.: Formation of toxic alkylbenzenes in edible oils submitted to frying
682 temperature. Influence of oil composition in main components and heating time, *Food Res. Int.*,
683 43(8), 2161–2170, doi:10.1016/j.foodres.2010.07.022, 2010.

684 Vicente, A. M. P., Rocha, S., Duarte, M., Moreira, R., Nunes, T. and Alves, C. A.: Fingerprinting
685 and emission rates of particulate organic compounds from typical restaurants in Portugal, *Sci. Total*
686 *Environ.*, 778, 146090, doi:10.1016/J.SCITOTENV.2021.146090, 2021.

687 Wang, G., Cheng, S., Wei, W., Wen, W., Wang, X. and Yao, S.: Chemical characteristics of fine
688 particles emitted from different chinese cooking styles, *Aerosol Air Qual. Res.*, 15(6), 2357–2366,
689 doi:10.4209/aaqr.2015.02.0079, 2015.

690 Wang, H., Guo, S., Yu, Y., Shen, R., Zhu, W., Tang, R., Tan, R., Liu, K., Song, K., Zhang, W.,

691 Zhang, Z., Shuai, S., Xu, H., Zheng, J., Chen, S., Li, S., Zeng, L. and Wu, Z.: Secondary aerosol
692 formation from a Chinese gasoline vehicle: Impacts of fuel (E10, gasoline) and driving conditions
693 (idling, cruising), *Sci. Total Environ.*, 795, doi:10.1016/j.scitotenv.2021.148809, 2021.

694 Wang, L., Zhang, L., Ristovski, Z., Zheng, X., Wang, H., Li, L., Gao, J., Salimi, F., Gao, Y., Jing, S.,
695 Wang, L., Chen, J. and Stevanovic, S.: Assessing the Effect of Reactive Oxygen Species and Volatile
696 Organic Compound Profiles Coming from Certain Types of Chinese Cooking on the Toxicity of
697 Human Bronchial Epithelial Cells, *Environ. Sci. Technol.*, 54(14), 8868–8877,
698 doi:10.1021/acs.est.9b07553, 2020.

699 Wei See, S., Karthikeyan, S. and Balasubramanian, R.: Health risk assessment of occupational
700 exposure to particulate-phase polycyclic aromatic hydrocarbons associated with Chinese, Malay and
701 Indian cooking, *J. Environ. Monit.*, 8(3), 369–376, doi:10.1039/b516173h, 2006.

702 Wu, W., Zhao, B., Wang, S. and Hao, J.: Ozone and secondary organic aerosol formation potential
703 from anthropogenic volatile organic compounds emissions in China, *J. Environ. Sci. (China)*, 53,
704 224–237, doi:10.1016/j.jes.2016.03.025, 2017.

705 Yi, H., Huang, Y., Tang, X., Zhao, S., Xie, X. and Zhang, Y.: Characteristics of non-methane
706 hydrocarbons and benzene series emission from commonly cooking oil fumes, *Atmos. Environ.*, 200,
707 208–220, doi:10.1016/j.atmosenv.2018.12.018, 2019.

708 Yu, Y., Wang, H. H. H., Wang, T., Song, K., Tan, T., Wan, Z., Gao, Y., Dong, H., Chen, S., Zeng, L.,
709 Hu, M., Wang, H. H. H., Lou, S., Zhu, W. and Guo, S.: Elucidating the importance of semi-volatile
710 organic compounds to secondary organic aerosol formation at a regional site during the EXPLORE-
711 YRD campaign, *Atmos. Environ.*, 246, doi:10.1016/j.atmosenv.2020.118043, 2021.

712 Yu, Y., Guo, S., Wang, H., Shen, R., Zhu, W., Tan, R., Song, K., Zhang, Z., Li, S., Chen, Y. and Hu,
713 M.: Importance of Semivolatile/Intermediate-Volatility Organic Compounds to Secondary Organic
714 Aerosol Formation from Chinese Domestic Cooking Emissions, *Environ. Sci. Technol. Lett.*,
715 doi:10.1021/acs.estlett.2c00207, 2022.

716 Zeng, J., Yu, Z., Mekic, M., Liu, J., Li, S., Loisel, G., Gao, W., Gandolfo, A., Zhou, Z., Wang, X.,
717 Herrmann, H., Gligorovski, S. and Li, X.: Evolution of Indoor Cooking Emissions Captured by
718 Using Secondary Electrospray Ionization High-Resolution Mass Spectrometry, *Environ. Sci.*

719 Technol. Lett., 7(2), 76–81 [online] Available from:
720 <https://pubs.acs.org/doi/full/10.1021/acs.estlett.0c00044> (Accessed 19 July 2021), 2020.

721 Zhang, D. C., Liu, J. J., Jia, L. Z., Wang, P. and Han, X.: Speciation of VOCs in the cooking fumes
722 from five edible oils and their corresponding health risk assessments, *Atmos. Environ.*, 211, 6–17,
723 doi:10.1016/j.atmosenv.2019.04.043, 2019.

724 Zhang, X., Zhang, M. and Adhikari, B.: Recent developments in frying technologies applied to fresh
725 foods, *Trends Food Sci. Technol.*, 98, 68–81, doi:10.1016/j.tifs.2020.02.007, 2020.

726 Zhang, X. Y., Lu, Y., Du, Y., Wang, W. L., Yang, L. L. and Wu, Q. Y.: Comprehensive GC×GC-
727 qMS with a mass-to-charge ratio difference extraction method to identify new brominated
728 byproducts during ozonation and their toxicity assessment, *J. Hazard. Mater.*, 403,
729 doi:10.1016/j.jhazmat.2020.124103, 2021a.

730 Zhang, Z., Zhu, W., Hu, M., Wang, H., Chen, Z., Shen, R., Yu, Y., Tan, R. and Guo, S.: Secondary
731 Organic Aerosol from Typical Chinese Domestic Cooking Emissions, *Environ. Sci. Technol. Lett.*,
732 8(1), 24–31, doi:10.1021/acs.estlett.0c00754, 2021b.

733 Zhao, Y. and Zhao, B.: Emissions of air pollutants from Chinese cooking: A literature review,
734 Tsinghua University Press., 2018.

735 Zhao, Y., Hu, M., Slanina, S. and Zhang, Y.: Chemical compositions of fine particulate organic
736 matter emitted from Chinese cooking., 2007a.

737 Zhao, Y., Hu, M., Slanina, S. and Zhang, Y.: The molecular distribution of fine particulate organic
738 matter emitted from Western-style fast food cooking, *Atmos. Environ.*, 41(37), 8163–8171,
739 doi:10.1016/j.atmosenv.2007.06.029, 2007b.

740 Zhao, Y., Hennigan, C. J., May, A. A., Tkacik, D. S., De Gouw, J. A., Gilman, J. B., Kuster, W. C.,
741 Borbon, A. and Robinson, A. L.: Intermediate-volatility organic compounds: A large source of
742 secondary organic aerosol, *Environ. Sci. Technol.*, 48(23), 13743–13750, doi:10.1021/es5035188,
743 2014.

744 Zhao, Y., Saleh, R., Saliba, G., Presto, A. A., Gordon, T. D., Drozd, G. T., Goldstein, A. H.,
745 Donahue, N. M. and Robinson, A. L.: Reducing secondary organic aerosol formation from gasoline
746 vehicle exhaust, *Proc. Natl. Acad. Sci. U. S. A.*, 114(27), 6984–6989, doi:10.1073/pnas.1620911114,

747 2017.

748 Zhao, Y., Lambe, A. T., Saleh, R., Saliba, G. and Robinson, A. L.: Secondary Organic Aerosol
749 Production from Gasoline Vehicle Exhaust: Effects of Engine Technology, Cold Start, and Emission
750 Certification Standard, *Environ. Sci. Technol.*, 52(3), 1253–1261, doi:10.1021/acs.est.7b05045, 2018.

751 Zhu, W., Guo, S., Zhang, Z., Wang, H., Yu, Y., Chen, Z., Shen, R., Tan, R., Song, K., Liu, K., Tang,
752 R., Liu, Y., Lou, S., Li, Y., Zhang, W., Zhang, Z., Shuai, S., Xu, H., Li, S., Chen, Y., Hu, M.,
753 Canonaco, F. and Prévôt, A. S. H.: Mass spectral characterization of secondary organic aerosol from
754 urban cooking and vehicular sources, *Atmos. Chem. Phys.*, 21(19), 15065–15079, doi:10.5194/acp-
755 21-15065-2021, 2021.

756 Zushi, Y., Hashimoto, S. and Tanabe, K.: Nontarget approach for environmental monitoring by GC ×
757 GC-HRTOFMS in the Tokyo Bay basin, *Chemosphere*, 156, 398–406,
758 doi:10.1016/j.chemosphere.2016.04.131, 2016.

759

760

761 **Figure Captions:**

762 **Figure 1.** Chemical identified from fried chicken (a), Kung Pao chicken (b), Pan-fried tofu (c), and
763 stir-fried cabbage (d) emissions. Column and Tenax TA bleeding after 75 min in 1st retention time are
764 excluded from qualification, quantification, and 2D binning processes. Blobs are colored by
765 chemical groups.

766 **Figure 2.** Emission rate (ER), ozone formation potential (OFP), and secondary organic aerosol (SOA)
767 estimation from emissions of fried chicken, Kung Pao chicken, pan-fried tofu, and stir-fried cabbage.
768 The unit of the y-axis is $\mu\text{g min}^{-1}$.

769 **Figure 3.** Volatility-polarity panels of gaseous chemical emissions from fried chicken, Kung Pao
770 chicken, pan-fried tofu, and stir-fried cabbage fumes, and ozone formation potential (OFP), and
771 secondary organic aerosol (SOA) estimation from gas-phase precursors. VOCs (blue color in *x*-axis),
772 IVOCs (orange color in *x*-axis), and SVOCs (red color in *x*-axis) are displayed in volatility bins (a
773 decrease of volatility from B9 to B31) along with their polarity (an increase from P1 to P10 in *y*-axis).
774 The emission rate (ER) unit is $\mu\text{g min}^{-1}$.

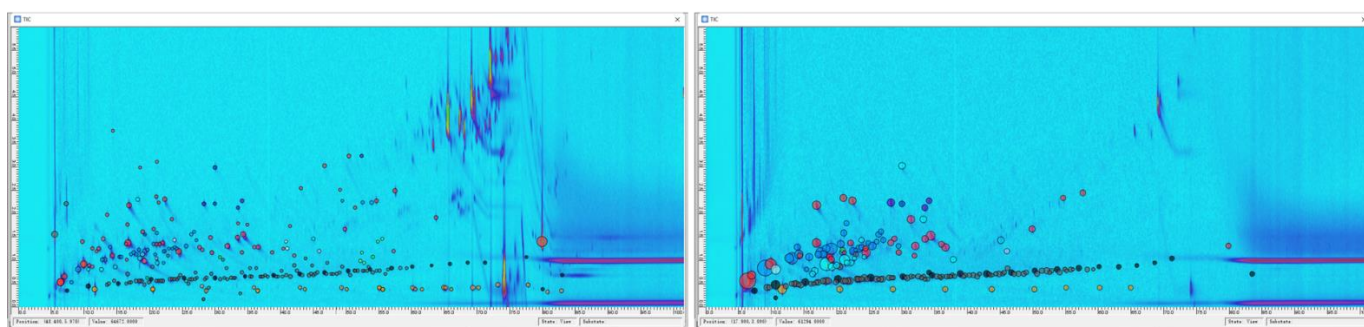
775 **Figure 4.** Emission rate (ER), ozone formation potential (OFP), and secondary organic aerosol (SOA)
776 estimation from emissions of fried chicken cooked with corn, peanut, soybean, and sunflower oils.
777 The unit of the y-axis is $\mu\text{g min}^{-1}$.

778 **Figure 5.** PLS-DA classification results in setting the cooking style (a) or oil (b) as grouping
779 variables. When oil was set as the grouping variable, the separation of groups was much better than
780 setting the dish as the grouping variable. The PLS-DA comparison result of cooking emissions and
781 oils is displayed in (c), indicating that the cooking fume is not just the evaporation of oil itself.
782 Positive loadings of oil and cooking fume chromatograms (d) demonstrated the key components
783 contributing to the similarities of samples.

784

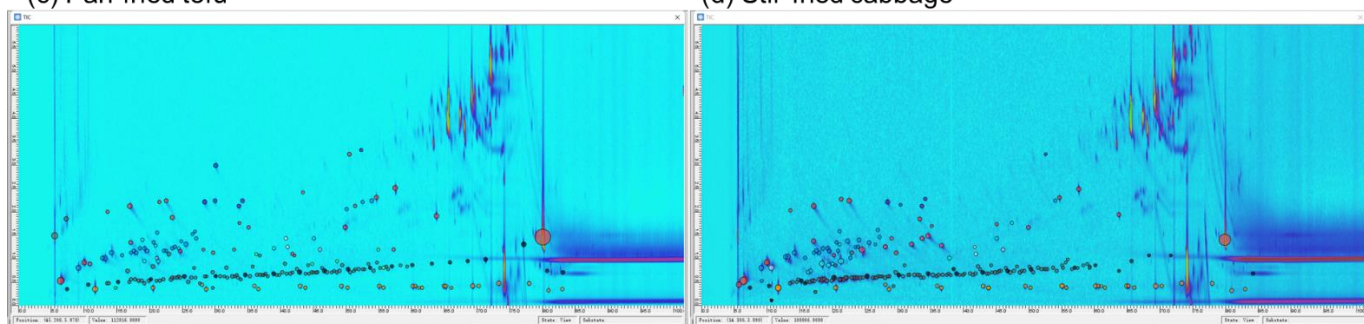
(a) Fried chicken

(b) Kung Pao chicken



(c) Pan-fried tofu

(d) Stir-fried cabbage

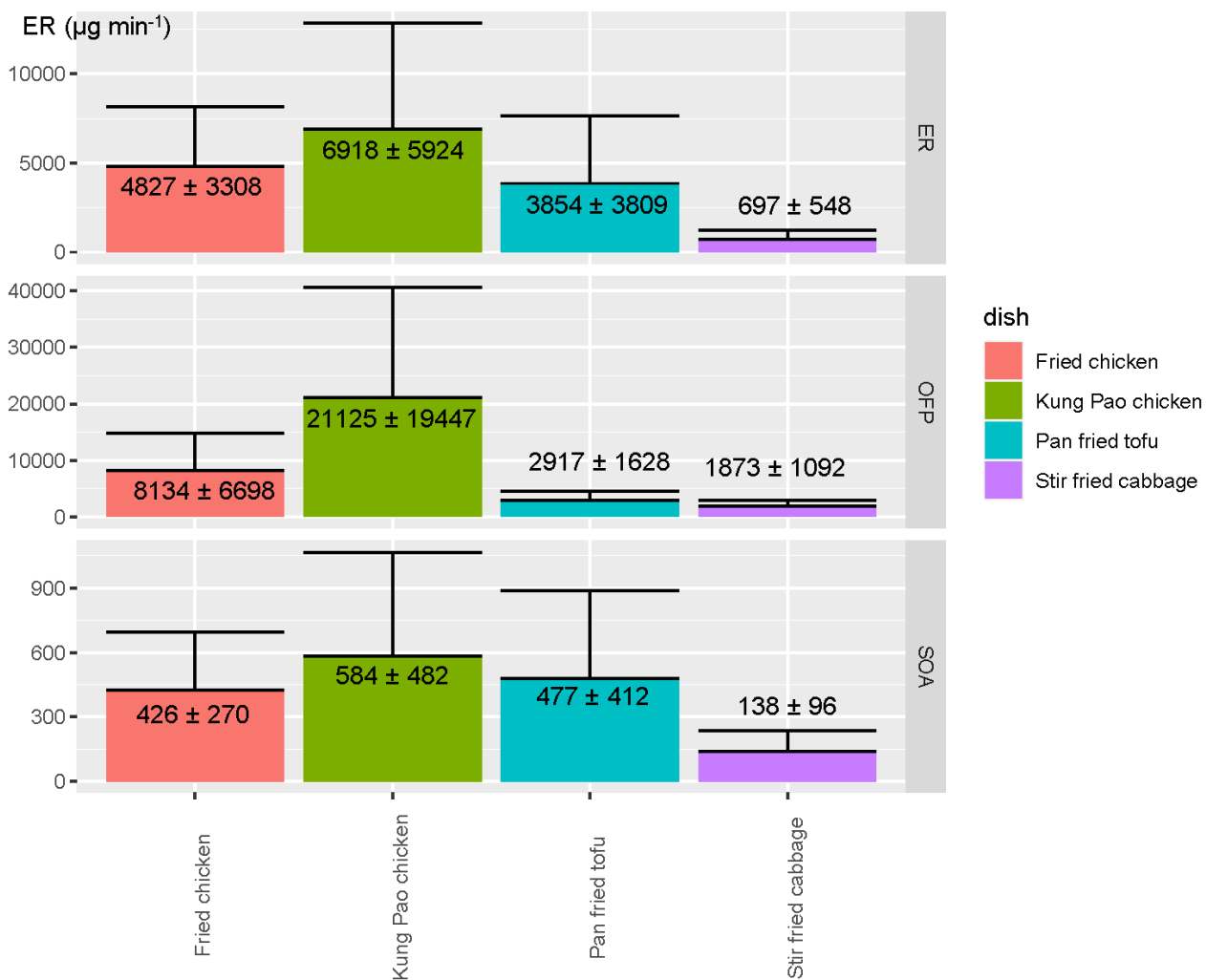


n-alkanes *b*-alkanes oxygenated compounds aromatics PAHs siloxanes alkenes others

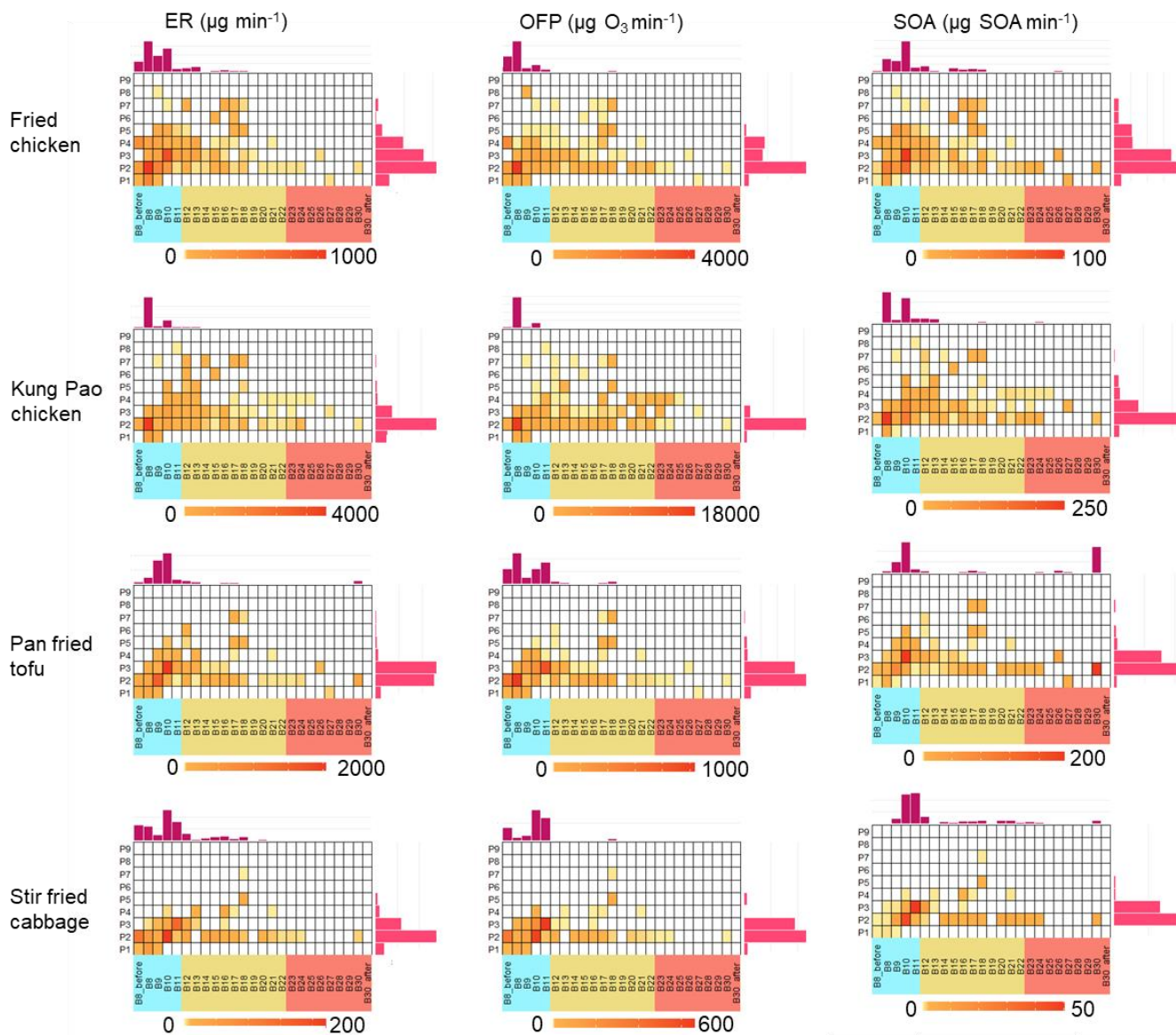
785

786 **Figure 1.** Chemical identified from fried chicken (a), Kung Pao chicken (b), Pan-fried tofu (c), and
787 stir-fried cabbage (d) emissions. Column and Tenax TA bleeding after 75 min in 1st retention time are
788 excluded from qualification, quantification, and 2D binning processes. Blobs are colored by
789 chemical groups.

790



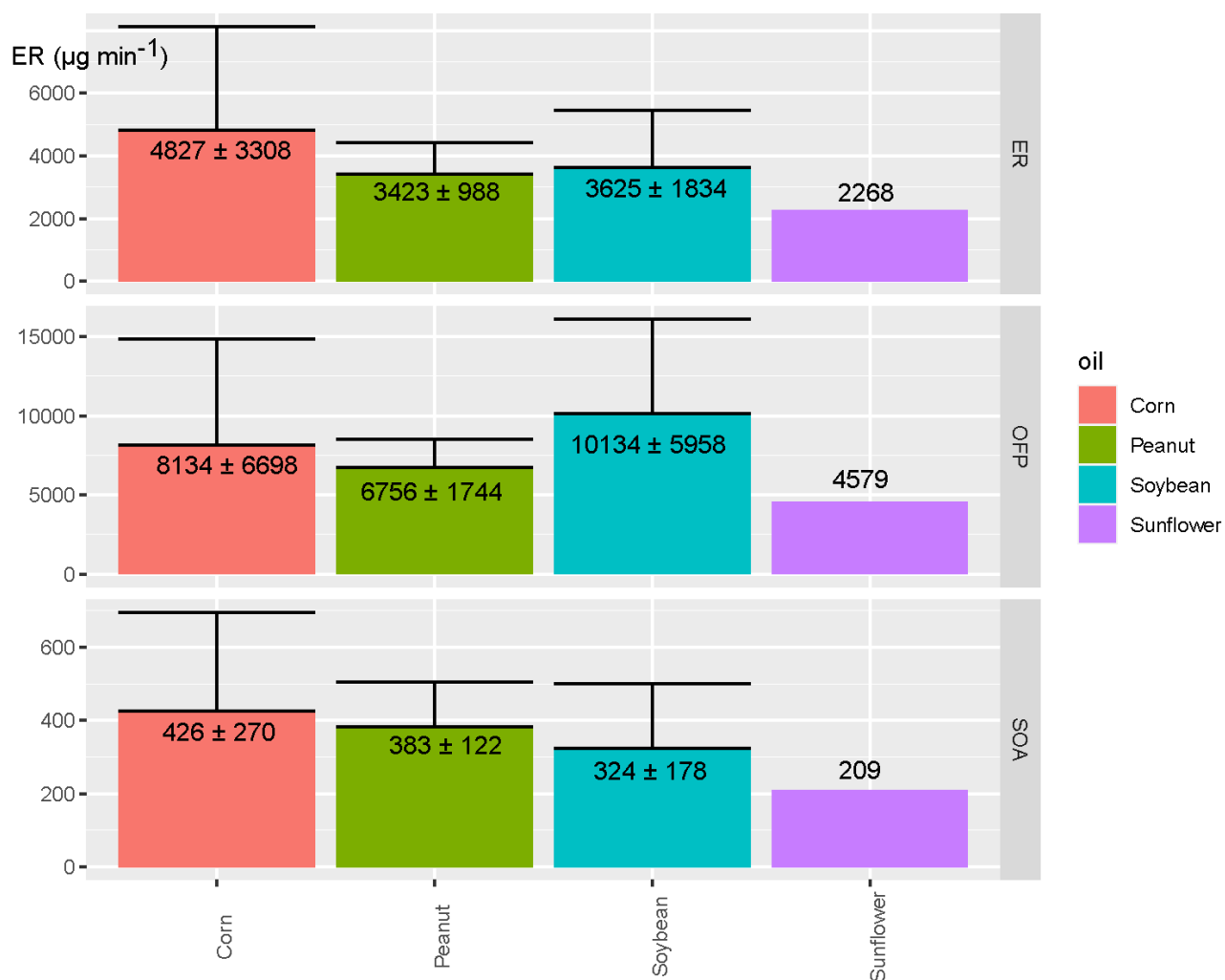
791
 792 **Figure 2.** Emission rate (ER), ozone formation potential (OFP), and secondary organic aerosol (SOA)
 793 estimation from emissions of fried chicken, Kung Pao chicken, pan-fried tofu, and stir-fried cabbage.
 794 The unit of the y-axis is $\mu\text{g min}^{-1}$.



795

796 **Figure 3.** Volatility-polarity panels of gaseous chemical emissions from fried chicken, Kung Pao
 797 chicken, pan-fried tofu, and stir-fried cabbage fumes, ozone formation potential (OFP), and
 798 secondary organic aerosol (SOA) estimation from gas-phase precursors. VOCs (blue color in *x*-axis),
 799 IVOCs (orange color in *x*-axis), and SVOCs (red color in *x*-axis) are displayed in volatility bins (a
 800 decrease of volatility from B9 to B31) along with their polarity (an increase from P1 to P10 in *y*-axis).
 801 The emission rate (ER) unit is $\mu\text{g min}^{-1}$.

802



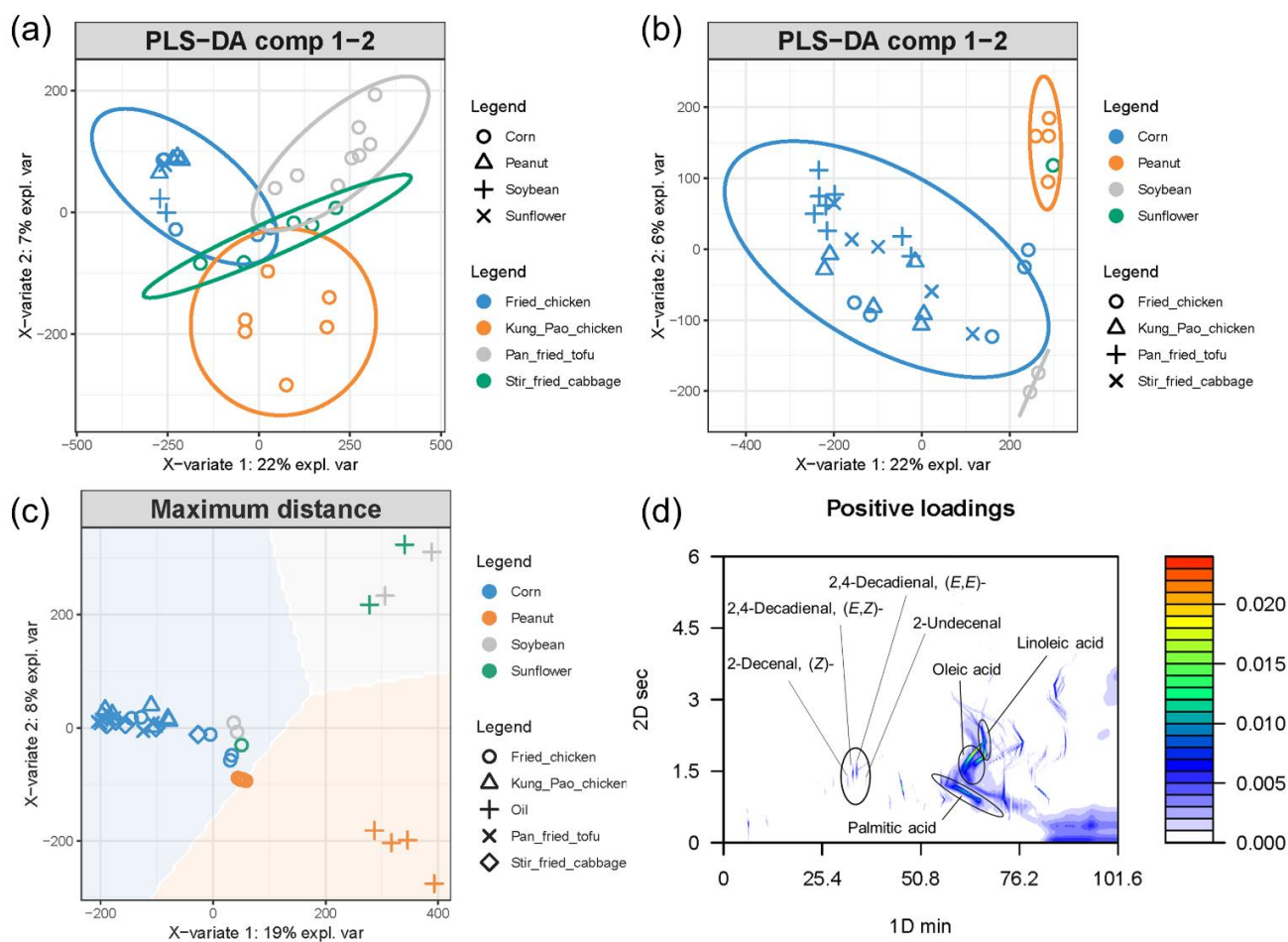
803

804 **Figure 4.** Emission rate (ER), ozone formation potential (OFP), and secondary organic aerosol (SOA)

805 estimation from emissions of fried chicken cooked with corn, peanut, soybean, and sunflower oils.

806 The unit of the y-axis is $\mu\text{g min}^{-1}$.

807



808

809 **Figure 5.** PLS-DA classification results in setting the cooking style (a) or oil (b) as grouping
 810 variables. When oil was set as the grouping variable, the separation of groups was much better than
 811 setting the dish as the grouping variable. The PLS-DA comparison result of cooking emissions and
 812 oils is displayed in (c), indicating that the cooking fume is not just the evaporation of oil itself.

813 Positive loadings of oil and cooking fume chromatograms (d) demonstrated the key components
 814 contributing to the similarities of samples. The color bar in (d) is the positive loading of pixels.

815